## NACA

## RESEARCH MEMORANDUM

THE EFFECTS OF WING-MOUNTED EXTERNAL STORES ON THE TRIM,

BUFFET, AND DRAG CHARACTERISTICS OF A ROCKET-PROPELLED

MODEL HAVING A 45° SWEPTBACK WING

By Allen B. Henning

Langley Aeronautical Laboratory Langley Field, Va.

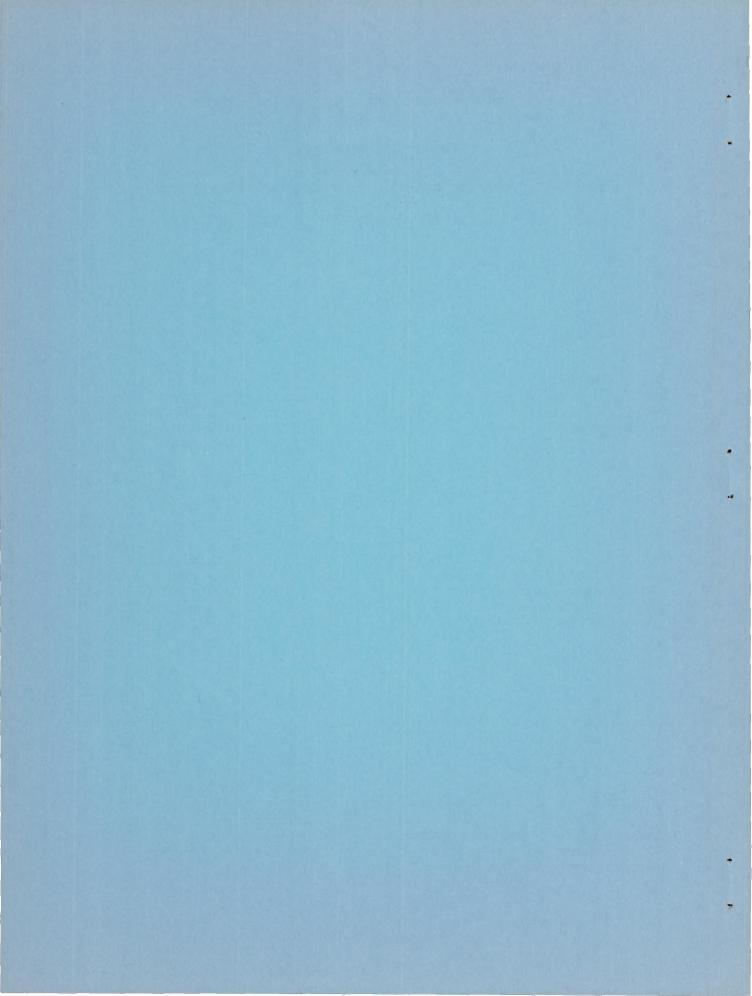
CLASSIFIED DOCUMENT

This material contains information affecting the National Defense of the United States within the meaning of the espionage laws, Title 18, U.S.C., Secs. 793 and 794, the transmission or revelation of which in any manner to an unauthorized person is prohibited by law.

# NATIONAL ADVISORY COMMITTED FOR AERONAUTICS

WASHINGTON

April 22, 1954



### NATIONAL ADVISORY COMMITTEE FOR AERONAUTICS

### RESEARCH MEMORANDUM

THE EFFECTS OF WING-MOUNTED EXTERNAL STORES ON THE TRIM,

BUFFET, AND DRAG CHARACTERISTICS OF A ROCKET-PROPELLED

MODEL HAVING A 45° SWEPTBACK WING

By Allen B. Henning

### SUMMARY

A rocket-propelled model has been flown to determine the effects of four wing-mounted bomb-type external stores on the trim, buffet, and drag characteristics of a wing-fuselage configuration having a 45° sweptback wing. The data are compared with data from a similar model without stores. The 45° sweptback wing had an aspect ratio of 3.56, a taper ratio of 0.3, and NACA 64A007 airfoil sections. Also, in conjunction with this test, a model has been flown by the helium-gun technique to obtain the drag of one isolated store.

The results of these tests are presented herein as the variation of trim angle of attack, trim normal—, and transverse-force coefficients, wing-tip helix angles, normal and transverse buffet intensities, and drag coefficients with Mach number. With the addition of external stores to the wing-fuselage configuration, there is a large drag increase, a nose-up trim change, and a slight decrease in buffet intensities above M=1.0 caused by the presence of the stores.

### INTRODUCTION

It has been common procedure to place external stores on aircraft operating in the subsonic speed range and the characteristics of external stores at these speeds are well-known. In contrast to that, little is known about the transonic and supersonic aerodynamic characteristics of externally mounted stores. This paper is a report on the flight results obtained from mounting four bomb-type stores on a 45° sweptback wing of a rocket-propelled model and a comparison of these results with data procured from a similar model without external stores (ref. 1). Included in this paper are the results of drag measurements on an isolated store model flown by the helium-gun technique.

### SYMBOLS

А	cross-sectional area, sq ft
al	longitudinal acceleration, g units
an	normal acceleration, g units
ant	trim normal acceleration, g units
Ъ	wing span, ft
$c_{\mathrm{D}}$	drag coefficient, $\frac{\text{Drag}}{\text{qS}}$
$\Delta C_{\mathrm{D}}$	increment of drag coefficient due to stores
$C_{m_{CL}}$	static longitudinal stability parameter
$C^{\mathbb{N}}$	normal-force coefficient, $\frac{\text{Normal force}}{\text{qS}}$
$c_{N_{\alpha}}$	slope of lift curve
$c_{ m N_T}$	trim normal-force coefficient
${\rm C}_{\Upsilon_{\underline{T}}}$	trim side-force coefficient, $\frac{\text{Side force}}{\text{qS}}$
Δg	increment of acceleration due to buffeting
L	length of body, ft
M	Mach number
р	rolling velocity, radians/sec
q	dynamic pressure, lb/sq ft
R	Reynolds number
<u>5A</u>	wing-tip helix angle, radians

S total wing area, sq ft

V velocity, fps

angle of attack, deg

mean aerodynamic chord of wing, 1.348 ft

h<sub>1</sub> first coast of model

ho second coast of model

### MODELS AND TESTS

### Models

The basic model used for this test was the same as the "tail-off" model of reference 1 and had no horizontal tail. Four identical bombtype stores were placed on the wing of the basic configuration in such a position as to give favorable flap and ground clearances. A drawing of the model and external stores showing the location of the stores and giving the principal dimensions and characteristics is shown in figure 1. The wing had an aspect ratio of 3.56, a taper ratio of 0.3, and NACA 64A007 airfoil sections. The center-of-gravity positions of the inboard and outboard stores were located at 0.0962 ahead of the mean-aerodynamicchord leading edge and 0.1572 behind the mean-aerodynamic-chord leading edge, respectively. The pylons between the stores and the model wing had NACA 65A006 airfoil sections and were unswept. An isolated-store model was flown in conjunction with this test to obtain the drag of the store alone. Photographs of the complete model and of the isolated-store model are shown as figure 2. A list of coordinates for the basic model body and the external store is given in table I and the longitudinal distribution of cross-sectional area is shown in figure 3.

The model was instrumented the same as the "tail-off" model of reference 1. An angle-of-attack indicator was sting-mounted on the nose of the model. Normal, transverse, and longitudinal accelerometers were mounted near the quarter chord of the wing root and normal and transverse accelerometers were mounted near the vertical tail root. The natural frequency of all the transverse and normal accelerometers was between 90 and 125 cycles per second and they were 55 to 65 percent critically damped. These characteristics along with the recorder characteristics produced amplitude-response factors varying from 0.7 to 1.0 at frequencies from 65 to 120 cycles per second.

### Tests

Shake tests were made in the laboratory to determine the natural frequencies and the modes of vibration of the wings. The results of these tests are presented in table II. The vertical-tail first-bending frequency was 130 cycles per second.

The model and booster combination mounted on the launcher prior to the model flight is shown in figure 4. The model was accelerated to M=1.4 by a 6-inch ABL Deacon rocket motor and then allowed to coast to M=0.8 at which time the sustainer fired and accelerated it to M=1.3. The data presented herein were measured during the coasting portions of the flight.

Data from the instruments in the model were transmitted to the ground and recorded by the standard NACA telemetering system. Flight-path data were obtained from SCR 584 tracking radar, velocity from CW Doppler radar set, and rate of roll from the spinsonde recorders by using the model telemetering antennas. Atmospheric data were obtained from a radiosonde instrument launched immediately after the test flight. The scale of these tests is shown by the plot of Reynolds number against Mach number in figure 5. The dynamic pressure is plotted against Mach number for each coasting period in figure 6. The first and second coasting periods are identified by h<sub>1</sub> and h<sub>2</sub>, respectively.

The isolated-store model (see fig. 2(b)) flown in conjunction with these tests was flight-tested by the helium-gun technique (ref. 2). The data from this flight were corrected for the difference in tail configurations of the stores. All flight tests were performed at the Langley Pilotless Aircraft Research Station at Wallops Island, Va.

#### ACCURACY

The following table presents the maximum probable error for  $\alpha$ ,  $C_N$ ,  $C_Y$ , and  $C_D$  due to instrument-calibration ranges:

					$M_{.} = 0.8$	M = 1.2
α,	de	eg			±0.5	±0.5
$c_{N}$					±.02	±.01
Cy					±.02	±.Ol
$c_{D}$					±.Ol	±.005

The instrument characteristics along with the recorder characteristics produced amplitude-response factors varying from 0.7 to 1.0 at frequencies from 65 to 120 cycles per second and the measured values of  $\Delta g$  due to buffeting were corrected accordingly. The minimum buffet amplitude that could be identified on the telemeter records was estimated to be approximately  $\pm 0.05g$  units. Mach numbers are estimated to be accurate within 1 percent at supersonic speeds and 2 percent at subsonic speeds.

### RESULTS AND DISCUSSION

Data from the test of a 45° swept-wing—fuselage configuration with 4 wing-mounted bomb-type external stores are shown and compared with data from reference 1 for a similar model without stores. The effects of the stores on the trim, buffet, lift, stability, and drag characteristics of the configuration are presented herein. All coefficients are based on the total wing area which includes the wing area within the fuselage.

### Trim

The variation of trim angles of attack, trim normal-force coefficients, trim side-force coefficients, and wing-tip helix angles with Mach number for the model with and without stores is shown in figure 7. The trim angles of attack and the normal-force coefficients show a large nose-up trim change with increasing speed starting near M=0.85 for the model with stores as compared with the nearly constant values for the model without stores. This large trim change, which is in a direction opposed to the pitching moment due to the store drag, would indicate that there is a large amount of interference between the stores and the model. The side-force coefficient and the wing-tip helix angle (fig. 7) showed very little change from the model with stores to the one without stores; therefore, the store interference is effective only in the normal plane.

### Buffet

Portions of the telemeter records showing the test flights for the model with stores and without stores at M=1.2 to 1.3 and also for the model with stores at M=0.92 to 0.95 are shown in figure 8. The model with stores does not show any buffeting near M=1.3 whereas the model without stores shows definite buffeting. The oscillations of the model with stores near M=1.3 are caused by the booster-model separation and near M=0.94 by the transonic change in trim. The oscillations from the booster-model separation show that, even though the model had a changing angle of attack, it does not have a tendency to buffet.

The normal buffet intensity at M=1.2, as shown in figure 9, does not appear in figure 8(b), which is the first coasting period, but this buffet does appear during the second coasting period. Slight buffeting of the stores model is indicated on the  $a_n$  traces at M=0.92 to M=0.95.

Mach number in figures 9 and 10. Addition of the stores has little effect on the normal buffet intensity or the transverse buffet intensity at Mach numbers up to 1.2. Above that speed, the addition of stores practically eliminates the buffet found for the basic configuration. Other effects observed were that the maximum transverse buffet intensities occurred near the wing root on the model without stores and near the tail root on the model with stores, the latter being more intense. The intensity near the wing root decreased with the addition of stores. The transverse buffet frequencies near the tail root for the model with stores is 117 cycles per second as compared with 85 cycles per second near the wing root whereas, for the model without stores, the frequency is 100 to 110 cycles per second for both locations. The data indicate that the addition of external stores had no appreciable adverse effects on the buffeting characteristics of this configuration.

### Lift and Stability

The variation of normal-force coefficient with angle of attack at supersonic speeds for the model with and without stores is shown in figure 11. There is no appreciable difference in  $C_{N_{\rm CL}}$  between the two configurations. The static longitudinal stability parameter  $C_{m_{\rm CL}}$  for the model with stores is -0.0168 at M = 1.3 with the center of gravity at 14.22 percent of the mean aerodynamic chord as compared with -0.018 at M = 1.3 for the model without stores with the center of gravity at 14.5 percent of the mean aerodynamic chord.

#### Drag

The drag coefficients for the model with and without stores are shown in figure 12(a). These data show a large increase in total drag over the test Mach number range and a decrease in the drag-rise Mach

number  $\left(M\right)$  where  $\frac{dC_D}{dM} = 0.1$  of 0.04 resulting from the addition of 4 stores.

The drag increment (fig. 12(b)) due to the addition of 4 stores is obtained by subtracting the store-off data from the store-on data. This incremental drag is compared with four times the drag of one isolated store obtained from the flight of the store-alone model. Four times the

drag of a similar store from reference 3 is also shown. The differences between  $\Delta C_D$  due to stores and the isolated store drag times four would indicate that there are large interference effects present between the stores and the model. Although the individual store drag plus interference from this model is high, it compares favorably with data from reference 4 which show that the interference between stores and airplane produce a high drag as compared with the stores alone.

For the purpose of possibly predicting the drag of this model a study was made by using the area-rule concept of reference 5 to find the peak pressure drag coefficient. This value was added to the subsonic drag coefficient to obtain the predicted peak drag coefficient. The predicted and experimental drag coefficients are tabulated in table III. The calculations were made for two different variations of the test configuration, namely, (1) a wing-body configuration without external stores, and (2) a wing-body configuration with four wing-mounted external stores. The calculations showed the peak pressure drag coefficient for both configurations to be much less than the experimental peak pressure drag coefficients. For example, on the model with stores, the predicted peak pressure drag coefficient as based on the wing area of the configuration was about 0.0175 compared with 0.0333 for the measured peak pressure drag coefficient. If the drag increments due to adding stores to the basic configuration are compared, it can be seen that the calculated  $\Delta C_D$ is 0.013 and the experimental  $\Delta C_D$  is 0.0173. From the above comparison and from the results of reference 2, it is apparent that, as yet, not enough is known about the area-rule concept to predict accurately the drag for swept-wing configurations of this type.

### CONCLUSIONS

A rocket-propelled model has been flown to determine the effects of four wing-mounted bomb-type external stores on the trim, buffet, and drag characteristics of a wing-fuselage configuration having a 45° swept-back wing. With the addition of four external stores to the reference model there was a large increase in drag of approximately 4 to 6 times that of the isolated store model and a decided nose-up trim change thought to be caused by strong interference between the stores and the model. The interference effects increased the drag by a large amount although the normal buffet intensity of the model was somewhat relieved.

Langley Aeronautical Laboratory,
National Advisory Committee for Aeronautics,
Langley Field, Va., February 9, 1954.

### REFERENCES

- 1. Mason, Homer P.: Flight Test Results of Rocket-Propelled Buffet-Research Models Having 45° Sweptback Wings and 45° Sweptback Tails Located in the Wing Chord Plane. NACA RM L53I10, 1953.
- 2. Hall, James Rudyard: Comparison of Free-Flight Measurements of the Zero-Lift Drag Rise of Six Airplane Configurations and Their Equivalent Bodies of Revolution at Transonic Speeds. NACA RM L53J2la, 1953.
- 3. Mitcham, Grady L., and Blanchard, Willard S., Jr.: Low-Lift Drag and Stability Data From Rocket Models of a Modified-Delta-Wing Airplane With and Without External Stores at Mach Numbers From 0.8 to 1.36. NACA RM L53A27, 1953.
- 4. Smith, Norman F., Bielat, Ralph P., and Guy, Lawrence D.: Drag of External Stores and Nacelles at Transonic and Supersonic Speeds. NACA RM L53I23b, 1953.
- 5. Nelson, Robert L., and Stoney, William E., Jr.: Pressure Drag of Bodies at Mach Numbers up to 2.0. NACA RM L53I22c, 1953.

TABLE I
TABLE OF COORDINATES

Fusel	age	Store		
Station	Radius	Station	Radius	
0 2.5 7.0 10.5 10.5 10.5 10.5 10.5 10.5 10.5 10	0 0.508 0.979 1.413 1.810 2.493 2.779 3.2416 3.556 3.750 3.750 3.680 3.5444 3.196 3.196 3.497 2.249 2.479 2.479 2.479 2.479 2.4438	0 0.328 0.796 1.265 1.733 2.202 2.670 3.139 3.607 4.076 4.544 5.013 5.481 5.959 7.167 8.385 8.854 9.322 9.791 10.259 10.728 11.196 11.665 12.133 12.602 13.070 13.538 14.007 14.475 14.944 15.412 15.787 16.162 16.537 16.865	0 0.160 .343 .484 .592 .677 .745 .800 .848 .889 .955 .976 .984 .980 .969 .952 .929 .900 .865 .824 .731 .679 .623 .565 .504 .442 .379 .328 .275 .204 0	

TABLE II NATURAL FREQUENCIES AND MODE SHAPES OF THE MODEL

First wing bending, cps	Second wing bending, cps	Wing torsion, cps	Intermediate wing bending, cps
	×=>(=>		× <u></u> Ō×
64	227	344	130 - 146

TABLE III

TOTAL SUPERSONIC DRAG CALCULATIONS

		Calcul	ated <sup>1</sup>	Experimental <sup>1</sup>	
Configuration	Frontal view	Peak pressure drag coefficient	Peak drag coefficient	Peak pressure drag coefficient	Peak drag coefficient
(1) Wing + body		0.011	0.022	0.0225	0.0335
(2) Wing + body + 4 stores	<del>- 50</del> 0 <del>00</del>	.0175	.035	.0333	.0508
Drag-coefficien	t increment	.0065	.013	.0105	.0173

lAll drag coefficients are based on the wing area.

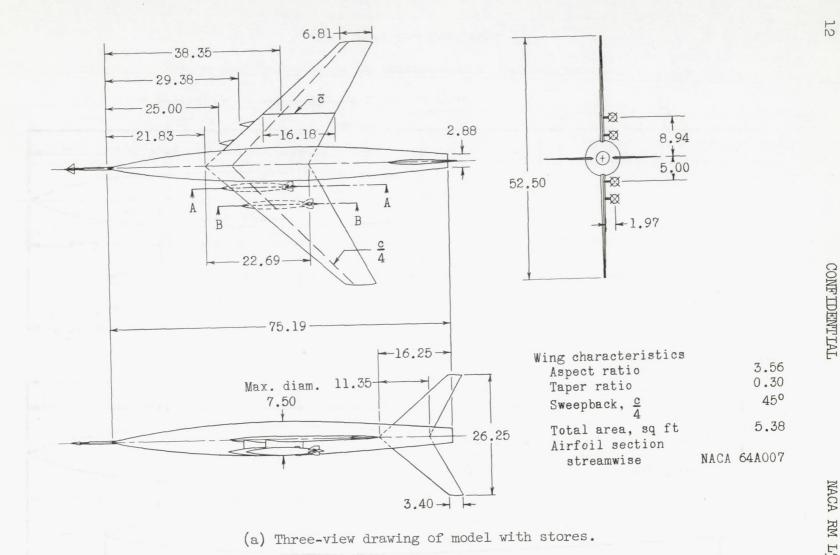
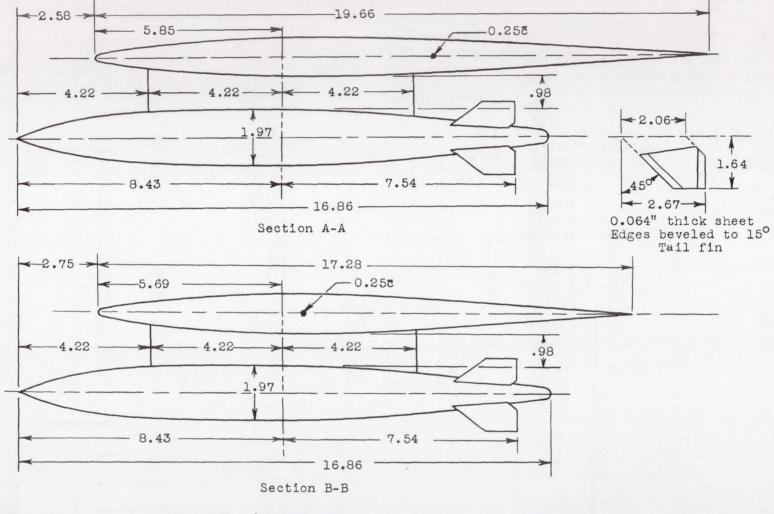
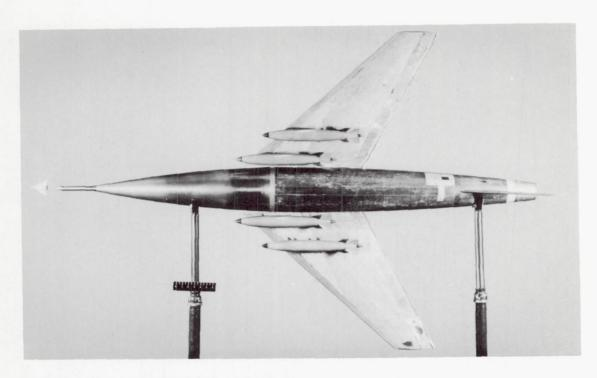


Figure 1.- Drawings showing dimensions and characteristics of test model. All dimensions are in inches.



(b) Details of external-store assemblies.

Figure 1.- Concluded.

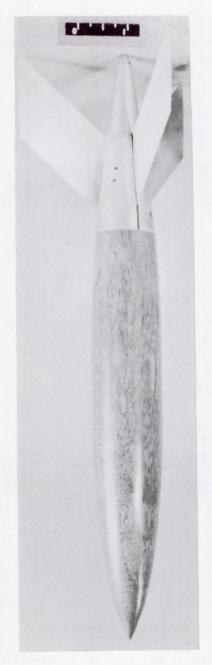




(a) Model showing external-store location.

L-83334

Figure 2.- Photographs of model and isolated-store model.



0-79426

Figure 2.- Concluded.

(b) Isolated store model.

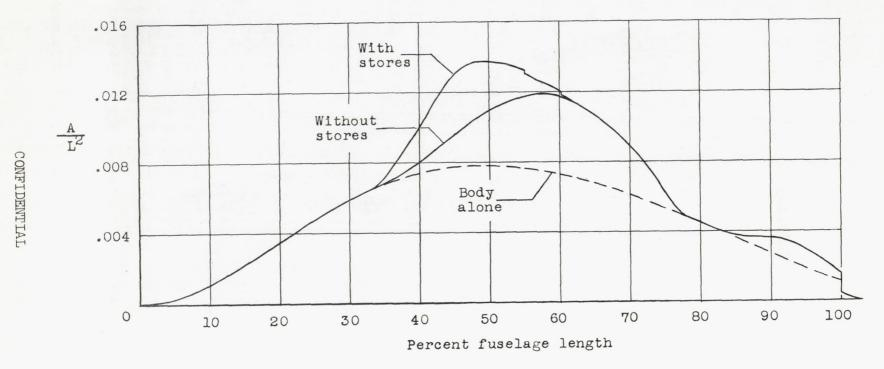


Figure 3.- Longitudinal distribution of cross-sectional area.



L-79988

Figure 4.- Photograph of model and booster on the launcher.

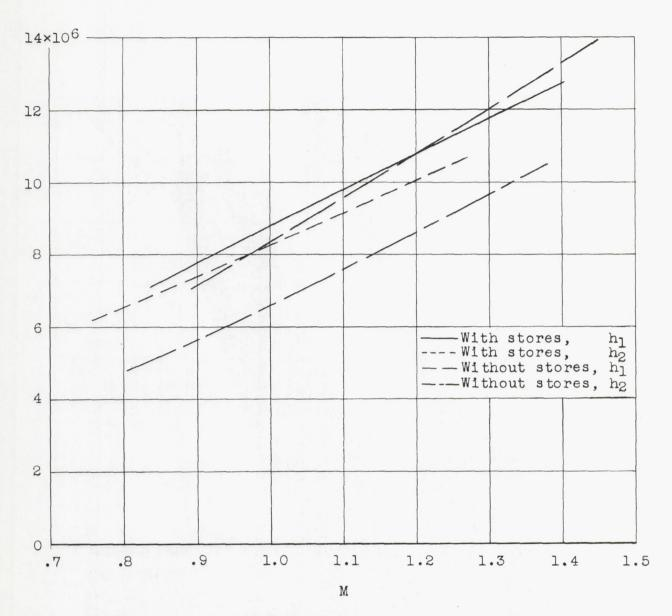


Figure 5.- Variation of Reynolds number, based on the wing mean aerodynamic chord, with Mach number.

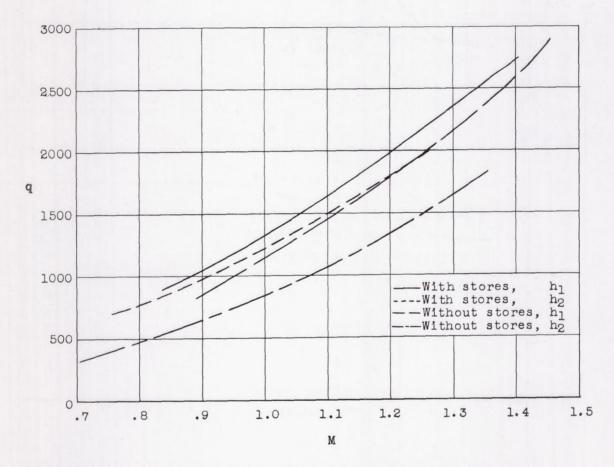


Figure 6.- Variation of dynamic pressure with Mach number.

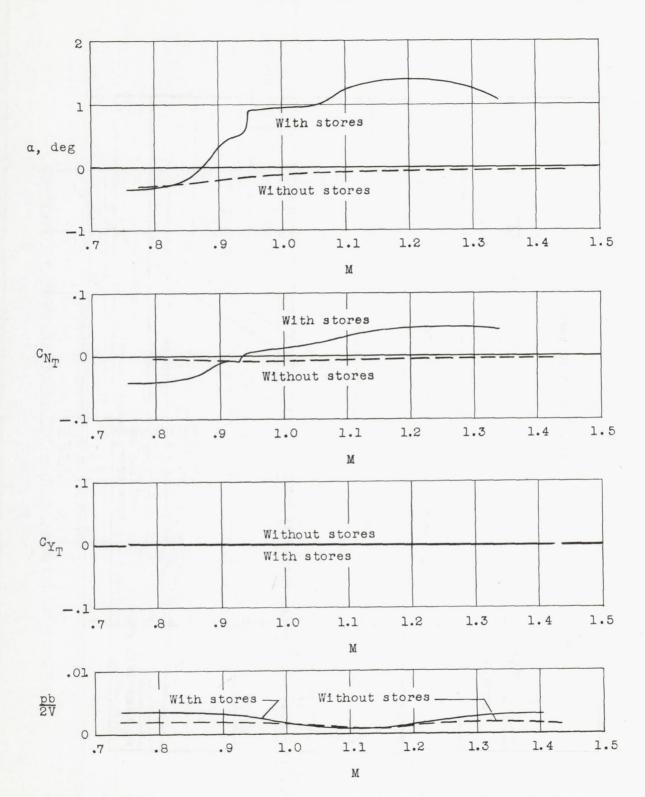
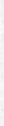
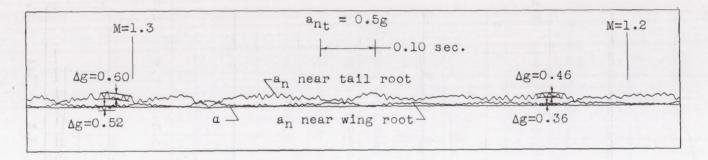
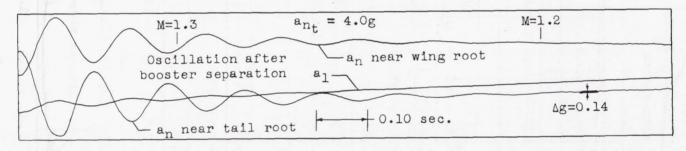


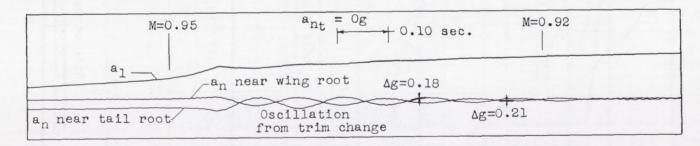
Figure 7.- Variation of trim angle of attack, trim normal- and side-force coefficients, and wing-tip helix angles with Mach number.





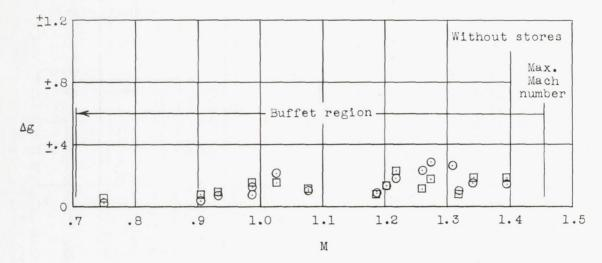
(a) Model without external stores.





(b) Model with external stores.

Figure 8.- Portions of telemeter records of normal acceleration.



- O Measured near wing root
- ☐ Measured near tail root

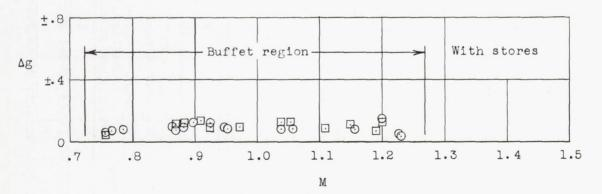
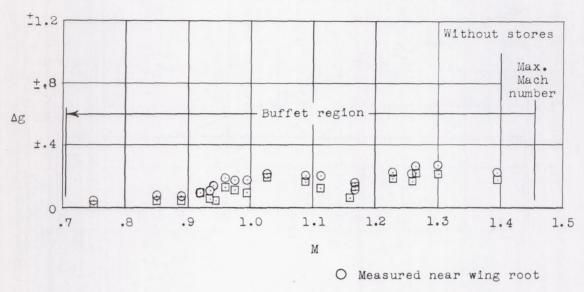


Figure 9.- Variation of normal buffet intensity with Mach number.



☐ Measured near tail root

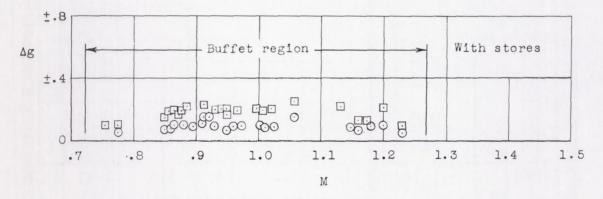
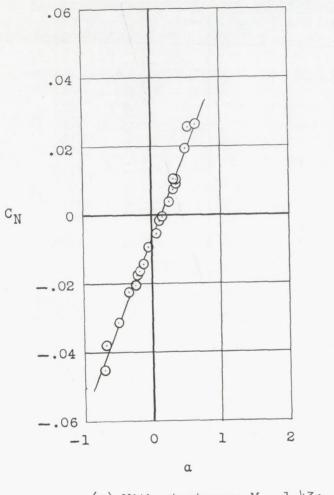
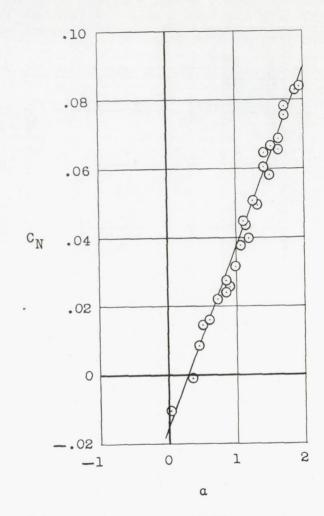


Figure 10.- Variation of transverse buffet intensity with Mach number.

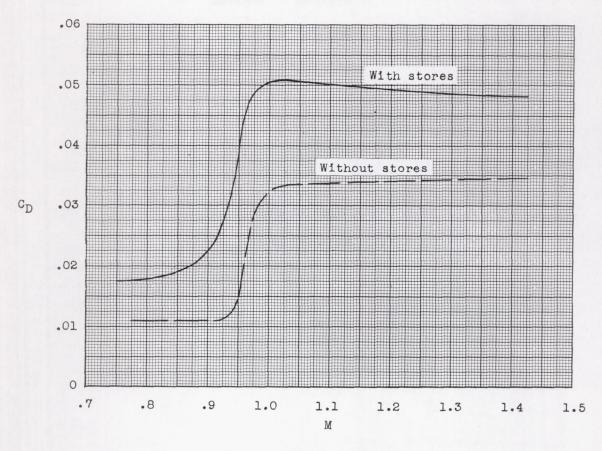




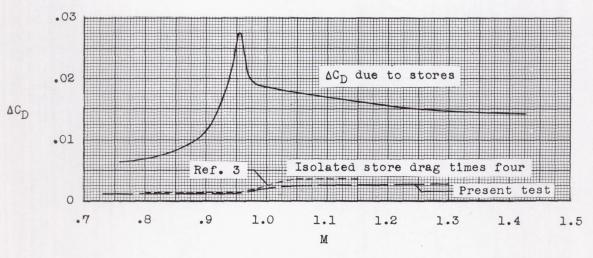


(b) With stores; M = 1.33;  $C_{N_{\alpha}} = 0.053$ .

Figure 11.- Variation of normal-force coefficient with angle of attack.



(a) Total drag coefficients.



(b) Incremental drag.

Figure 12.- Drag characteristics based on total wing area.

